Cellular Microbiology (2007) **9**(6), 1588–1600
doi:10.1111/j.1462-5822.2007.00895.x
First published online 16 February 2007

An extracellular matrix glues together the aerial-grown hyphae of *Aspergillus fumigatus*

Anne Beauvais,[1]* Christine Schmidt,[2] Stéphanie Guadagnini,[2] Pascal Roux,[3] Emmanuelle Perret,[3] Christine Henry,[1] Sophie Paris,[1] Adeline Mallet,[2] Marie-Christine Prévost[2] and Jean Paul Latgé[1]

[1]*Aspergillus Unit,* [2]*Electron Microscopy Platform and* [3]*Dynamic Imagery Platform, Institut Pasteur, Paris, France.*

Summary

Pulmonary infections due to *Aspergillus fumigatus* result from the development of a colony of tightly associated hyphae in contact with the air, either in the alveoli (invasive aspergillosis) or in an existing cavity (aspergilloma). The fungal ball observed *in vivo* resembles an aerial colony obtained in agar medium *in vitro* more than a mycelial mass obtained in liquid shaken conditions that have been classically used to date to study *A. fumigatus* physiology. For this reason, we embarked on an analysis of the characteristics of *A. fumigatus* colonies grown in aerial static conditions. (i) Under static aerial conditions, mycelial growth is greater than in shaken, submerged conditions. (ii) The colony surface of *A. fumigatus* revealed the presence of an extracellular hydrophobic matrix that acts as a cohesive linkage bonding hyphae into a contiguous sheath. (iii) The extracellular matrix is composed of galactomannan, α1,3 glucans, monosaccharides and polyols, melanin and proteins including major antigens and hydrophobins. (iv) *A. fumigatus* colonies were more resistant to polyenes than shake, submerged mycelium. This is the first analysis of the three dimensional structure of a mycelial colony. Knowledge of this multicellular organization will impact our future understanding of the pathobiology of aerial mold pathogens.

Introduction

Aspergillus fumigatus is a thermophilic opportunistic fungus that sporulates abundantly in nature. Pulmonary disease follows the inhalation of airborne conidia of *A. fumigatus* and colonization and invasion of the respiratory airway. Allergic bronchopulmonary aspergillosis (ABPA), aspergilloma and invasive pulmonary aspergillosis are among the most common and threatening pathologies due to *A. fumigatus*, which has become a leading cause of fungal morbidity and mortality in industrialized countries (Latgé, 2003).

Aspergilloma occurs in pre-existing pulmonary cavities and in chronically obstructed paranasal sinuses. Aspergilloma consists of a spheroid mass of hyphae that is in direct contact with air and may invade the entire cavity. Within the ball, hyphae are agglutinated and constitute a macrocolony of highly branched hyphal elements that are tightly associated. Invasive aspergillosis starts also with the development of an aerobic microcolony in the pulmonary alveoli. For a fungus, growing as a multicellular community may impart certain advantages to help colonize the substratum and resist external aggressions. In addition, an increasing number of studies show that the behaviour and physiology of cells isolated or belonging to a multicellular population are very different. Bacterial and yeast biofilms or flocculating yeasts are well-known examples of this phenomenon. Until now, many studies have described the polarization of the fungal expansion of isolated cells such as germinated conidia, hyphal septation and branching. But nobody has analysed how the hyphae or the yeast cells adhere together to form a colony, and the putative role of extracellular material in this cohesion. Moreover, all studies on *A. fumigatus* are performed with mycelium grown in liquid shake conditions (flasks, fermentor). No studies of the fungus grown *in vivo* in which the conditions are static and aerial have been undertaken. As the development of the fungus *in vivo* resembles an aerial colony grown on a solid substratum *in vitro*, studies of the morphological and physiological characteristics of the *in vitro* colony may help to understand the *in vivo* growth of this fungus.

We show for the first time that the growth characteristics vary for fungal colonies and pellets under aerial, static and submerged liquid culture conditions respectively. In addition, confocal microscopy and electron microscopy showed that the structures of the mycelial networks grown under these two conditions were also different. Finally, an extracellular matrix mainly composed of galactomannan and α1,3 glucan appears to envelop the hyphae as a complex matrix under aerial conditions.

Received 29 September, 2006; revised 26 December, 2006; accepted 2 January, 2007. *For correspondence. E-mail abeauvai@pasteur.fr; Tel. (+33) 1 45688225; Fax (+33) 1 40613419.

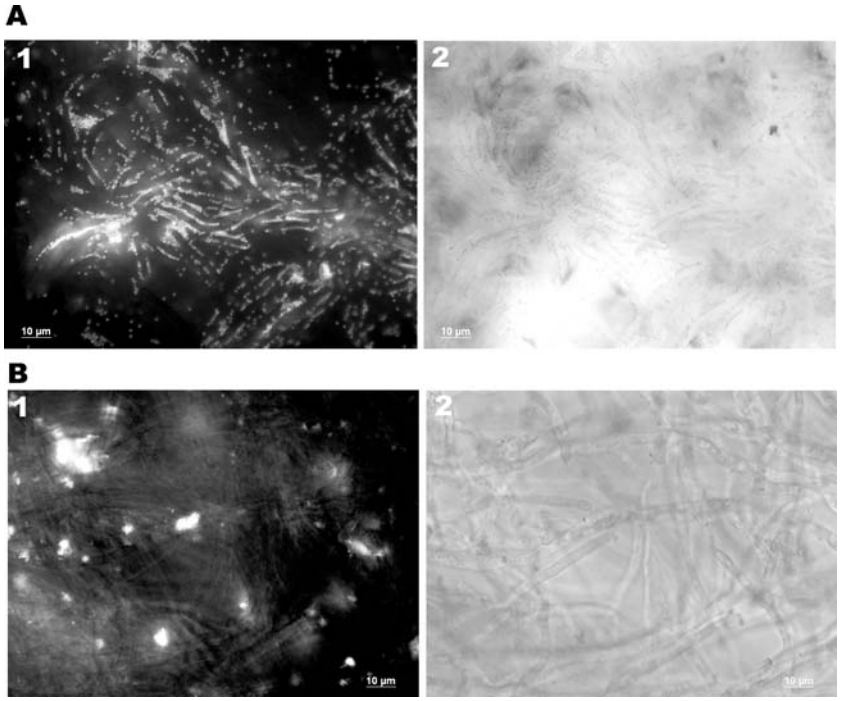

Fig. 1. Hydrophobicity of StA compared with ShS. The amount of attached polystyrene microspheres is much higher on StA hyphae (A) than on ShS hyphae (B), showing that StA are more hydrophobic than ShS. A1 and B1: epifluorescence; A2 and B2: Nomarsky light.

Results

Hydrophobicity of the mycelial colony

Mycelial mats grown under either static aerial (StA for Static Aerial) or submerged shake conditions (ShS for Shake Submerged) had different hydrophobic properties. When deposited on top of the colony, a drop of water was not dispersed on the StA mycelium. Opposite results were obtained with ShS mycelium. This difference in hydrophobicity was shown in a semiquantitative manner using polystyrene microbeads. The highest number of microspheres attached to the StA mycelium compared with the ShS confirmed that the StA colony was extremely hydrophobic (Fig. 1).

Growth of A. fumigatus *in the StA and ShS conditions*

The growth of *A. fumigatus* StA and ShS mycelia was quantified in 1% and 2% GYE media. In both media, the growth of the StA mycelium was greater and started earlier than the ShS mycelium (Fig. 2, and data not shown). After 16–17 h of growth in 1% GYE, the freeze-dried weight of the StA mycelium reached 0.65 (±0.01) mg ml^{-1}, whereas it was only 0.1 (±0.007) mg ml^{-1} in a ShS culture.

In 1% GYE, the stationary growth phase occurred after 39 h of culture in both conditions. At this time, the lyophilized weight of the mycelium from a StA culture was 1.5 times higher than from a ShS culture. Approximately one-third of the original glucose content of the culture medium remained unmetabolized in this medium after a 48 h culture (data not shown). This result suggested that the C/N ratio of the medium was unbalanced. To prevent this problem, the concentration of yeast extract was increased from 1% to 2% (2% GYE). This change induced a 1.6-fold increase in the mycelial weight of the StA condition (data not shown). After 48 h of growth in this medium, the freeze-dried weight of the StA mycelium (500 mg) was 2.5 times higher than in ShS mycelium (200 mg), and no more glucose could be detected in the medium of the StA culture. In contrast, in the ShS condition, growth remained unchanged in 1% and 2% GYE and 30% glucose remained present after 48 h growth in both media (data not shown).

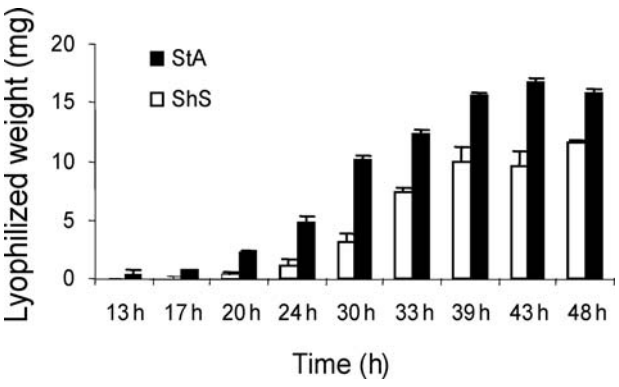

Fig. 2. Growth of StA and ShS mycelia in GYE 1% yeast extract from 13 h to 48 h.

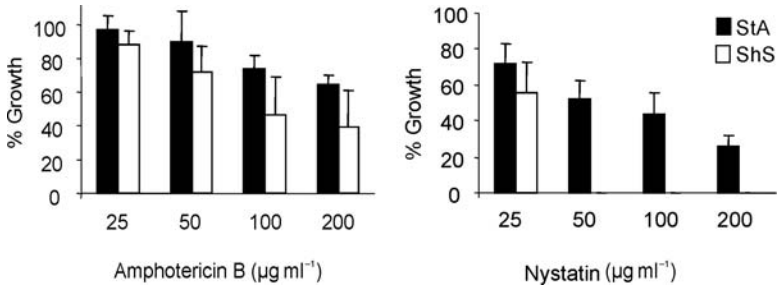

Fig. 3. Survival of StA or ShS mycelia at different concentrations of amphotericin B (left) and nystatin (right).

Antifungal, desiccation and temperature sensitivities to both growth forms

The efficacy of different antifungal agents was tested on the StA and ShS mycelia at different ages. A similar sensitivity to the imidazoles, itraconazole and voriconazole was observed for mycelia grown in the two culture conditions. The minimal 50% inhibitory concentration (MIC_{50}) was 8 μg ml^{-1} for itraconazole and 5 μg ml^{-1} for voriconazole (data not shown). The StA and ShS mycelia were as sensitive to caspofungin with a MIC_{50} of 0.4 μg ml^{-1} (data not shown).

In contrast, the sensitivity to the polyenes amphotericin B and nystatin was dependent on the culture conditions of the mycelium. The StA mycelium was the most resistant to the two drugs. After a 24 h incubation with 200 μg ml^{-1} amphotericin B, the growth of the StA mycelium was 46% inhibited while the ShS mycelium was 66% inhibited (Fig. 3). The difference was more pronounced with nystatin than with amphotericin B. The growth of the ShS mycelium was completely abolished after a pre-incubation of the mycelium with 50 μg ml^{-1} nystatin. The StA mycelium was still able to grow at 200 μg ml^{-1} nystatin (Fig. 3). Removal of the extracellular material by gentle rubbing of the surface did not modify the resistance to nystatin (see Fig. 5E; data not shown).

The StA mycelium was as sensitive to desiccation and heat as the ShS mycelium (data not shown).

Morphology

The morphology and structure of the StA mycelium were analysed by confocal and apotome microscopy, cryo-scanning (SEM) and transmission (TEM) electron microscopy. The thickness of the mycelial StA colony reached 20–30 μm after 16 h growth and 100–150 μm after 24 h (data not shown). After germination of the conidia on agar (10 h), the StA mycelium started to grow vertically to the surface of the colony (Fig. 4B). The vertically polarized growth provided an explanation for the depth of the network and the presence of channels between groups of hyphae (Fig. 4A). The extracellular material surrounding the mycelium was observed after calcofluor white staining (Fig. 4C). Epifluorescence microscopy revealed that this material prevented the calcofluor staining of embedded hyphae, whereas the ShS hyphae were labelled (Fig. 4D). This material was present at the surface of the culture after 20 h of growth (Fig. 4B).

Cryo-SEM observations confirmed that the network of StA hyphae was covered by a contiguous film (Fig. 5A). Almost undetectable after 16 h of growth, it increased in thickness with the age of the culture (Fig. 5B). High magnification showed that the surface of the film displayed a granular structure (Fig. 5C). When observed individually, hyphae were shown to be covered by an extracellular slime (Fig. 5D). The extracellular material that covers the surface of the colony is also seen between hyphae where it apparently glues together the hyphal threads of the network (Fig. 6). TEM confirmed the presence of channels observed by confocal microscopy (Fig. 6A). The electron-dense extracellular matrix was thicker on the surface of the colony than inside the colony (Fig. 6A).

In contrast, at all growth times tested, the ShS mycelium was totally devoid of any extracellular matrix (Fig. 7A), and the hyphal surface looked smooth (Fig. 7B). TEM observation confirmed the absence of an extracellular material linking the hyphae together and showed only the presence of a very thin electron-dense material at the cell wall surface (Fig. 7C).

Hyphae growing in the lung of immunocompromised mice experimentally infected with *A. fumigatus* were also covered by an extracellular matrix (Fig. 8).

Analysis of the StA extracellular material composition

Hexoses and polyols. Eighteen per cent (±5%) mannitol, 74% (±6%) glucose, 3% (±1.4%) trehalose and 5% (±2.7%) glycerol composed the total monosaccharide-polyol fractions of the extracellular matrix. Surprisingly, glucose was present in high concentration in the matrix secreted by the StA mycelium. All hexoses and polyols were found intracellularly in the same proportion as extracellularly (data not shown). We verified that glucose was also secreted into the extracellular matrix when the StA mycelium was growing in a medium without glucose (yeast extract 1% only) (data not shown). This result shows that the glucose recovered was not from the culture medium.

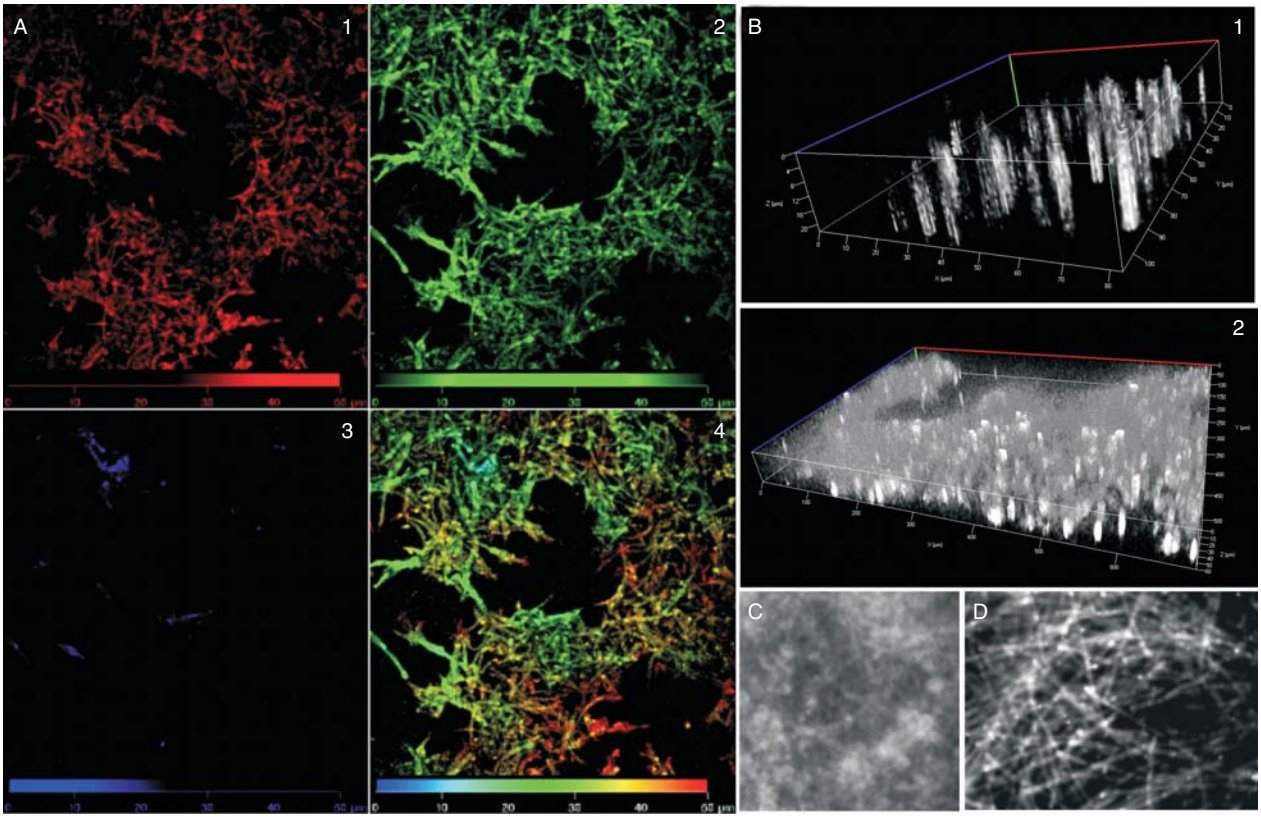

Fig. 4. Confocal and apotome microscopy images of *A. fumigatus* StA cultures.
A. Depth projection from confocal image stack recorded from StA after calcofluor white staining; 24 h growth, Plan-Apochromat 20×/0.75. A1 to A3 panels are sections of a 24 h StA culture from the agar surface (in red) to the air surface (blue). A4 is a reconstitution of A1 to A3.
B. Three-dimensional images of StA, Plan-Neofluar 40× (NA = 0.8) showing the vertical growth of the fungus (16 h growth, B1), followed by the appearance of extracellular material holding the hyphae together (24 h growth, B2)
C and D. Calcofluor white staining of StA (C) and ShS (D) mycelia showing the extracellular matrix covering the StA hyphae and preventing their staining in contrast to ShS hyphae which are stained (phase contrast, ×100).

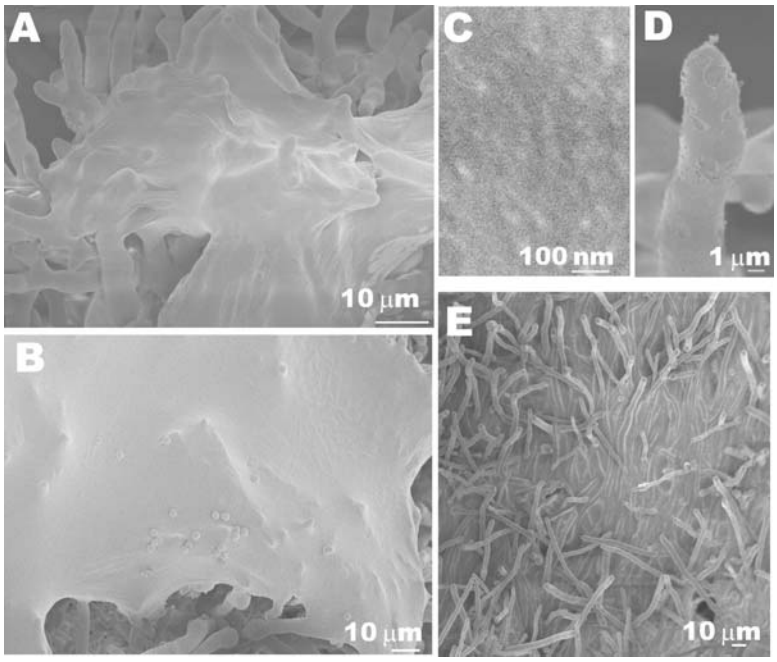

Fig. 5. Cryo-SEM images of StA mycelia of *A. fumigatus*.
A and B. Note the extracellular matrix covering the hyphae at the surface of the colony (24 h growth, A) and increasing with the age of the culture (30 h growth, B).
C. High magnification of the extracellular matrix.
D. Individual hyphae showing the presence of material covering the cell wall.
E. Appearance of StA mycelia after gentle rubbing of the surface with a policeman. Note the absence of the extracellular material covering the hyphae and the apparent absence of damage to the hyphae (24 h growth).

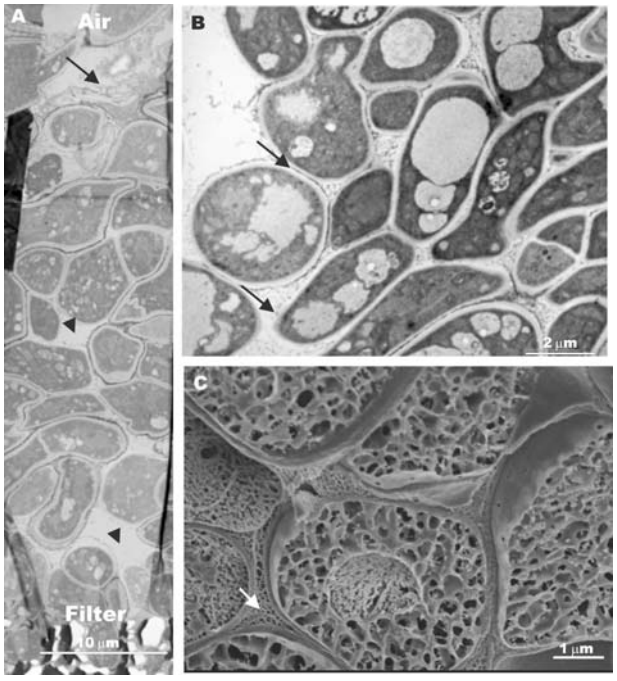

Fig. 6. Ultrastructure of StA mycelium of *A. fumigatus* (24 h growth).
A. Reconstituted section of the StA mat showing that all cells are active metabolically with air channels present in the colony mat (arrowhead) and the thicker extracellular material at the air surface (arrow).
B. High magnification of the network of hyphae showing the electron-dense extracellular material on the surface of the cell wall (arrows).
C. Cryo-SEM section showing the reticulate structure of the extracellular material (arrow) holding the hyphae together.

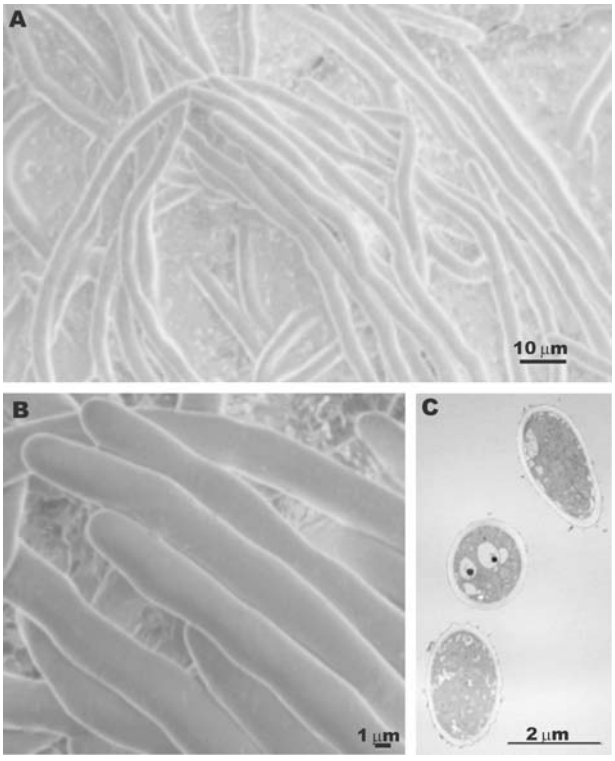

Fig. 7. Cryo-SEM (A and B) and TEM (C) images of ShS mycelium (30 h growth). Note the absence of extracellular material at the surface of hyphae on both Cryo-SEM and TEM microscope.

Galactomannan and α1,3 glucans. Immunoassays performed with anti-galactomannan monoclonal antibody showed an intense labelling of the extracellular matrix (Fig. 9A). Comparatively, immunolabelling of the mycelium of a ShS culture showed a total lack of labelling of the thin extracellular material when present at the surface of some hyphae (Fig. 9A). The presence of galactomannan in the matrix was confirmed by gas chromatography after recovering the extracellular material by gentle rubbing of the surface of a StA culture, ethanol precipitation and polysaccharide analysis as described in *Experimental procedures* (data not shown). Immunoassays also showed the presence of galactomannan in the cell wall

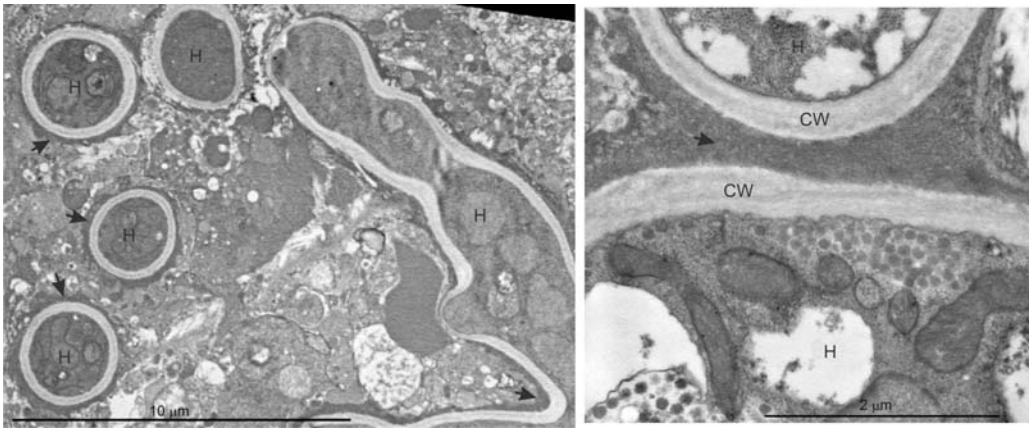

Fig. 8. Ultrathin section hyphae growing in the lung parenchyma of an experimentally infected mouse. Note the presence of an extracellular material (arrows) at the surface of the hyphae (H). CW, cell wall.

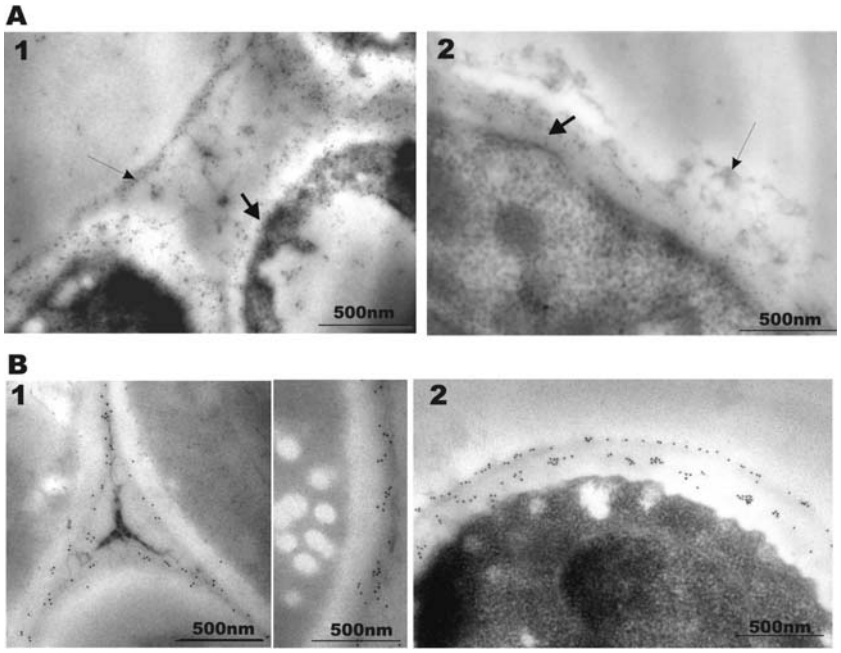

Fig. 9. Immunolabelling of the extracellular matrix (thin arrow) and the cell wall (thick arrow) of StA (1) and ShS (2) hyphae with anti-galactomannan (A) and anti-α1,3 glucan (B) antibodies. Note the absence of labelling of the thin extracellular material present at the surface of the ShS hyphae (A2) demonstrated with anti-galactomannan antibodies and the different localization of the immunolabelling in StA (B1) and ShS (B2) hyphae with the anti-α1,3 glucan antibodies.

and intracellular matrix of the StA and ShS mycelia as described previously (Stynen *et al*., 1992) (Fig. 9A). This was consistent with the analysis of the cell wall composition in which a similar amount of galactomannan (14%) was present in the StA and ShS cell wall (data not shown).

Ultrathin sections incubated with anti-α1,3 glucan antibodies showed a highly labelled, electron-dense amorphous material at the surface of the cell wall of StA mycelium, whereas the internal cell wall was not labelled (Fig. 9B). In contrast, two layers, a thin outer and an intermediate one, were labelled in the cell wall of the ShS mycelium (Fig. 9B). The presence of α1,3 glucan in the matrix was also confirmed chemically by gas chromatography (data not shown). In spite of a different distribution, cell wall analysis showed the same amount of α1,3 glucan in the StA and ShS mycelia (40%, data not shown). Incubation of the StA colony with α1,3 glucanase did not modify its resistance to polyenes (data not shown).

Galactomannan and α1,3 glucans accounted for 27% of the total hexose present in the extracellular matrix. Neither β1,3 glucans nor hexosamines were recovered in the StA matrix after gentle rubbing of the surface of a StA culture, ethanol precipitation and polysaccharide analysis, or β1,3 glucanase digestion (data not shown).

Proteins. The extracellular matrix contained 2% protein, including the three major secreted antigens of *A. fumigatus*, dipeptidylpeptidase V (DPPV), catalase B (CatB) and ribotoxin (ASPF1) (Fig. 10). The highly hydrophobic nature of the StA culture surface suggested also the presence of hydrophobic proteins in the StA extracellular matrix. Hydrophobins are surface active proteins produced by filamentous fungi that are found to be associated to aerial growth (Linder *et al*., 2005). In *A. fumigatus*, six hydrophobins, RodAp (Afu5g 09580), RodBp (Afu1g 17250), RodCp (Afu8g 07060), RodDp (Afu5g 01490), RodEp (Afu8g 05890) and RodFp (Afu5g 03280), have been identified in the genome. The open reading frame sequences are 480 bp, 423 bp, 468 bp,

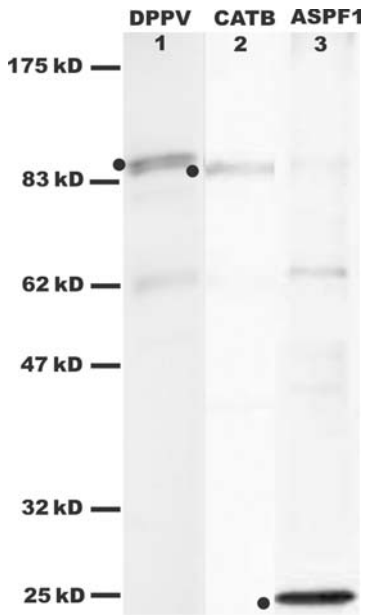

Fig. 10. Western blot of an SDS-PAGE of the extracellular matrix extract labelled with anti-DPPV (lane 1), anti-CatB (lane 2) and anti-ASPF1 (lane 3) antibodies.

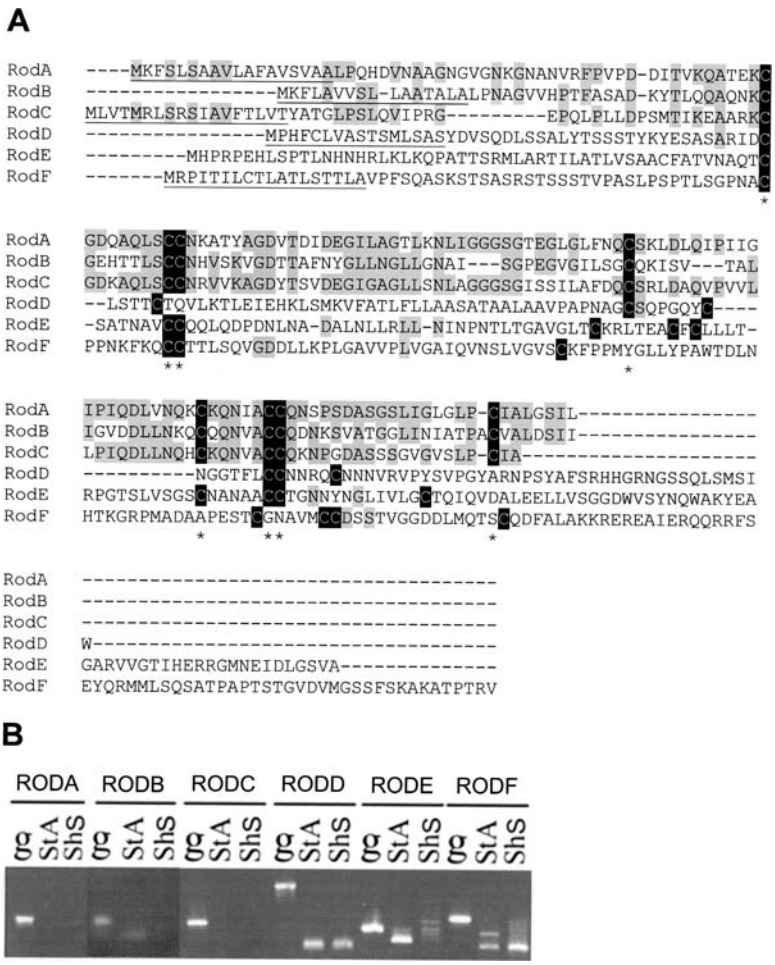

Fig. 11. Molecular analysis of hydrophobin genes.
A. Sequence alignment of the six *A. fumigatus* hydrophobin genes. The peptide signals are underlined and the conserved cysteine residues are box-shaded. Note the high homology (50%) between RodAp, RodBp and RodCp and the low homology of singletons RodDp, RodEp and RodFp with the RodA-Cps.
B. Analysis of expression of the six *ROD* genes in StA and ShS mycelia by RT-PCR. The primers used for each *ROD* genes were listed in *Experimental procedures*; g = genomic DNA used as positive control to indicate that a PCR product was amplified with these primers; the presence of a PCR band seen in the lane StA and lane ShS indicated that the respective *RODA-F* genes were expressed. Note the differences in size of the PCR product amplified from genomic and cDNA due to the presence of intron(s) in the genomic DNA flanked by the PCR primers.

579 bp, 438 bp and 636 bp respectively. They encode predicted proteins with estimated molecular masses of 14–17 kDa. Sequence analysis showed that like RodAp, RodBp, RodCp, RodEp and RodFp belong to class I hydrophobins (Wösten and de Vocht, 2000). RodBp is a typical class I hydrophobin characterized by eight conserved cysteine residues and the conserved spacing of hydrophilic and hydrophobic regions (Paris *et al*., 2003) (Fig. 11A). RodBp, like the two other typical hydrophobins RodAp and RodCp, displayed all the consensus sequences characteristic of the GPI-anchored proteins (Gerber *et al*., 1992) (S. Paris and J.P. Latgé, unpubl. results). RodEp is not a typical hydrophobin: RodEp has no signal peptide and a hydrophilic N-terminal region, 11 cysteine residues and a long-amino-acid end after the last cysteine (Fig. 11A). RodBp is 50% similar to RodAp and RodCp, whereas RodEp has no sequence homology (Fig. 11A). Of the six hydrophobins, reverse transcription polymerase chain reaction (RT-PCR) experiments showed that *RODA* and *RODC* were not expressed during vegetative growth. *RODD* and *RODF* mRNA were both present in the StA and ShS mycelium. Most interestingly, *RODB* and *RODE* mRNA were only found in the StA mycelium (Fig. 11B).

Melanin. Ultrathin sections of a StA culture showed the presence of an electron-dense material, very similar in appearance to the melanin present in the outer layer of the conidia cell wall. This material remained electron-dense in the absence of uranyl acetate/lead citrate staining of the ultrathin sections (Fig. 12). The presence of melanin in the extracellular material was confirmed by chemical extraction after hydrolase digestion, denaturation and HCl hydrolysis of the StA mycelium as described below (data not shown).

Discussion

The colony surface of *A. fumigatus* grown under aerial conditions revealed the presence of a hydrophobic matrix that cohesively bonds hyphae into a contiguous sheath. This matrix increases with the age of the culture. A colony of *A. fumigatus* grown in an aerial environment resembles bacteria or yeast biofilms, which are defined as a struc-

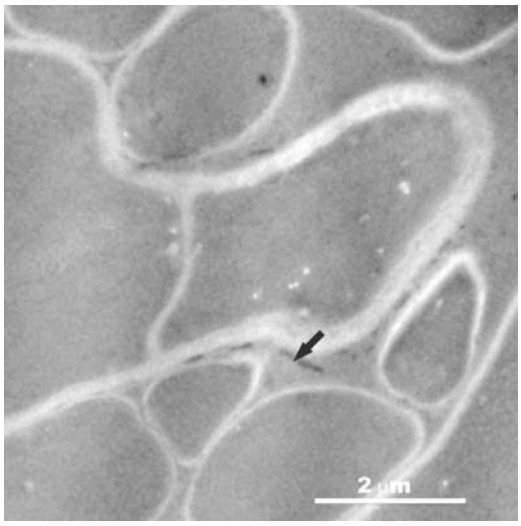

Fig. 12. Ultrathin section of the StA mycelium observed without uranyl acetate/lead citrate staining showing the presence of melanin (arrow) between cells.

tured microbial community of cells enclosed in an exopolysaccharide matrix (Lewis, 2001; Douglas, 2003). By this criterion, the StA state of *A. fumigatus* can therefore be called a fungal biofilm. Yet, an *A. fumigatus* biofilm (StA) differs in many aspects from a typical *Candida albicans* or bacterial biofilm. First, localization of the source of nutrients is opposite, as the upper layer of the biofilm is in contact with air and the lower one with nutrients. In yeast or bacterial biofilms, the lower layer is attached to the catheter or other plastic devices and has poor access to nutrients. Second, in bacterial biofilms, cells located in the upper regions are metabolically active and have a normal size, whereas cells unmeshed within the matrix are dormant and smaller in size (Anwar *et al*., 1992). *Candida* biofilms are composed of a three-dimensional structure consisting of microcolonies surrounded by water channels. Microcolonies of predominantly yeast forms are produced in the early phase, whereas the later phases show the formation of hyphae and pseudohyphae (Ramage and Lopez-Ribot, 2005). No such dimorphism exists in an *A. fumigatus* colony as hyphae appear morphologically similar and metabolically active from the agar surface towards the air. Channels are observed between groups of hyphae, but they are more likely involved in air circulation. The presence of these air channels could be at the origin of the oxidation mechanisms responsible for the production of melanin, identified for the first time in aerial hyaline mould hyphae. The nature of this melanin is unknown to date. Preliminary high-performance liquid chromatography (HPLC) experiments showed that it is not DHN-melanin (K. Dadachova and A. Casadevall, pers. comm.). Moreover, RT-PCR experiments showed that enzymes involved in pigment biosynthesis such as the polyketide synthase (*PKSP*) and the laccase (*ABR2*) encoding genes were not expressed during the StA growth (data not shown). However, Sugareva *et al*. (2006) showed that in an Δ*abr2* mutant strain, additional laccases are active during vegetative growth of *A. fumigatus*. In the genome of *A. fumigatus*, there are at least three additional candidate genes coding for potential laccases (Afu1g15670, Afu4g14280, Afu2g17540; http://www.tigr.org). The melanin present in the extracellular matrix of the StA culture could be synthesized by one of them. Finally, bacterial and yeast biofilms grow slowly because of the limited availability of nutrients, whereas an *A. fumigatus* biofilm has a biomass 1.5-fold greater than the ShS culture.

Other characteristics are shared between *A. fumigatus* colonies and yeast / bacterial biofilms. First, in *C. albicans* and in *A. fumigatus*, an extracellular matrix characterizes the intermediate development phase, whereas in *Cryptococcus neoformans*, exopolysaccharidic material is observed during the early maturation phase (Chandra *et al*., 2001; Martinez and Casadevall, 2006). Second, in all microorganisms, the biofilm is composed by polysaccharides. In *Staphylococcus epidermidis*, a linear β1,6 glucosaminoglycan comprises 75% of the biofilm matrix (Mack *et al*., 1996). The composition of the matrix in *C. albicans* biofilm is still largely unknown. It has been reported to contain 41% carbohydrate, including 16% glucose, which is the most abundant monosaccharide in the biofilm (Baillie and Douglas, 2000). Interestingly, the presence of free glucose was reported in the biofilm of both *C. albicans* and *A. fumigatus*. In *A. fumigatus*, it could be seen as a nutrient sliding along the extracellular matrix and being able to provide nutrients to the cells more distally located from the agar surface. In *A. fumigatus*, the matrix also contained high amounts of galactomannan and α1,3 glucan, which are also cell wall polysaccharides; galactomannan has been shown to be secreted in the culture filtrate (Stynen *et al*., 1992). These two polysaccharides are specific to the extracellular matrix as β1,3 glucan and hexosamines (chitin and polygalactosamine) were not found in the matrix biofilm.

The difference in environmental growth conditions has led to a different localization of these polysaccharides in the cell wall that favours their integration in the biofilm matrix. In the ShS cell wall, the α1,3 glucans are present at the surface and in a distinct central layer of the cell wall, whereas in the biofilm, amorphous α1,3 glucans were only observed at the surface of the cell wall in a thicker layer. This location suggests a close association with construction of the exopolysaccharide matrix, as well as with the galactomannan that has been shown to be associated to α1,3 glucans (W. Morelle, A. Beauvais and J.P. Latgé, unpubl. results).

Third, biofilms are also composed of a small amount of protein, 5% in *C. albicans* and 2% in *A. fumigatus*. The

identity of these proteins is unknown in both fungi. Our study demonstrated the presence of at least three major *A. fumigatus* antigens in the biofilm. The enzymes DPPV, catalase and ribonuclease (ASPF1), are recognized by aspergilloma patient sera, an indication that they are secreted *in vivo* as they are in an *in vitro* formed colony mat (Sarfati *et al*., 2006).

We were not able to identify rodlet proteins in the *A. fumigatus* biofilm following extractions by fluorohydric acid or trifluoroacetic acid (Paris *et al*., 2003) or using monospecific antibodies (data not shown). Yet, expression studies have shown that at least two of these hydrophobins are transcribed specifically in the StA mycelium. The construction of a Δ*rodB*–Δ*rodE* double mutant is currently underway to verify the role of these hydrophobins in biofilm formation and hydrophobicity of the colonial mat. Hydrophobic proteins have been reported to be important for the formation of aerial hyphae in other fungi. In *Schizophyllum commune*, the Sc3p class I hydrophobin is secreted at the surface of the cell wall of aerial hyphal elements (Wösten *et al*., 1999). This hydrophobin self-assembles in a rodlet structure at the interface between the hydrophilic cell wall and air. In *Ustilago maydis*, the *REP1* gene encodes a prepro-protein cleaved to 10 repeats of 34–55 hydrophobic amino acids and one longer peptide (228 aa), which are known as repellents. Eight are identified in the cells walls of aerial hyphae and the disruption of *REP1* results in a reduction of aerial hyphal formation (Wösten *et al*., 1996). However, no homologues of the repellents have been found in the *A. fumigatus* genome. In aerial hyphae of *Streptomyces tendae* and *S. coelicolor* two hydrophobic peptides steptofactin and SapB are secreted (Richter *et al*., 1998; Tillotson *et al*., 1998).

Finally, another specific characteristic of biofilms is their resistance to antimicrobial agents. A majority of recurrent infections caused by bacteria or yeast are associated with the formation of biofilms. Removal of the device that is supporting the biofilm growth is almost always required to eliminate the infection. Generally, bacteria embedded in a biofilm are 10–1000 times more resistant to antibiotics than are the planktonic cells (Donlan and Costerton, 2002). Similar results are reported for *C. albicans*, *C. parapsilosis* and *C. neoformans*. Resistance to azole antifungal drugs, including new triazoles, and to polyenes has been reported for biofilms, whereas echinocandin drugs show similar antifungal activity against planktonic or biofilms of *Candida* (Douglas, 2003). *A. fumigatus* colonies are more resistant to amphotericin B and nystatin than ShS mycelium but are as sensitive to triazole drugs and the echinocandin caspofungin. Following the methodology adapted from Ramage and Lopez-Ribot (2005) for *C. albicans* biofilm resistance to antifungal drugs, and plating the sheets of *A. fumigatus* mycelium in GYE medium, higher MIC_{50} were obtained compared with the classical method for antifungal susceptibility testing of filamentous fungi (NCCLS document M38-A, 2002). Slow growth of bacterial biofilms has been reported to be a major factor in the increased resistance to killing (Lewis, 2001). Many antibiotics have an absolute requirement for cell growth in order to kill, where the rate of killing is proportional to the rate of growth. However, this is not true for *C. albicans* and *A. fumigatus* biofilms as the same resistance is seen at all growth rates tested (Douglas, 2003) (data not shown). The reduced permeability of the extracellular matrix delays penetration of the drugs into the cells. The negatively charged β1,4 glucosaminoglycan of *S. epidermidis* is very effective in protecting cells from positively charged aminoglycoside antibiotics (Lewis, 2001). The role of the extracellular matrix of the *A. fumigatus* colony in delaying the penetration of the drugs is still unknown but preliminary experiments following the method described by Samaranayake *et al*. (2005) have shown that the penetration of nystatin through the ShS mycelium is higher than through the StA colony (data not shown). Briefly, a blank antibiotic disk was placed on the top of StA or ShS cultures which are incubated at the surface of a nystatin solution. The disk is then deposited on an agar plate spread plated with *Saccharomyces cerevisiae.* The halo of inhibition of growth of yeast is an indication of the diffusion of nystatin through the StA or ShS mycelium to the disk. The preliminary results show an absence of penetration through the StA mycelium whereas inhibitory zones were observed using the ShS mycelium at 100 and 200 μg ml^{-1} nystatin concentrations (data not shown). High expression of multidrug resistance efflux pumps (MDR) that transport antimicrobials has been demonstrated in yeast and bacterial biofilms (Anwar *et al*., 1992; Brooun *et al*., 2000; Maira-Litran *et al*., 2000; Lewis, 2001; Ramage *et al*., 2002; Garcia-Sanchez *et al*., 2004). Many MDR transporters, including ATP-binding cassettes and major facilitator superfamilies, have been identified in the *A. fumigatus* genome (Tekaia and Latgé, 2005). Transcriptome analysis of *A. fumigatus* growing under StA or ShS conditions is currently underway to identify biofilm-specific genes.

The correlation between the colony formed *in vitro* and *in vivo* in an alveoli remains to be established. Immunolabelling of the extracellular material present at the surface of the hyphae in the mice aspergillosis with antibodies directed against galactomannan and α1,3 glucan would confirm that this matrix is secreted by the fungus, as these polysaccharides are absent in mammals. These studies are currently underway.

Experimental procedures

Strains and culture conditions

Wild-type *A. fumigatus* ATCC 46645 was used in this study. This strain was maintained on 2% malt agar slants. Mycelium was

grown in 150 ml flasks containing 20 ml of liquid GYE medium (3% glucose, 1% yeast extract) shaken at 150 r.p.m. (ShS culture) or in 90 mm Petri dishes containing 20 ml of GYE agar medium covered by cellophane (DryEase cellophane, Invitrogen) or a Durapore filter (Millipore) (StA culture). Flasks and Petri dishes were inoculated with 2×10^7 conidia in 100 μl of a 0.01% Tween 20 aqueous solution and incubated at 30°C. Homogenous partition of the conidial inoculum for the StA culture was obtained by spreading the conidial suspension over the membrane with a policeman.

Experimental murine aspergillosis

Three male Swiss mice (40 g) were immunocompromised by intraperitoneal injections of cortisone acetate (10 mg per mouse on days −3, 0, +2). At day 0, they were infected with 10^7 *A. fumigatus* conidia (in 25 μl of phosphate-buffered saline-0.01% Tween 20) intranasally. When mice appeared moribund, animals were sacrificed and the lungs were fixed in 2.5% glutaraldehyde in 0.1 M Na cacodylate buffer for 2 h under vacuum at room temperature and overnight at 4°C. Fixed lungs were then processed for TEM as described below.

Growth measurements

Fungal growth was quantified at 30°C, in liquid media, GYE or GYE supplemented with 2% yeast extract instead of 1%. Under static conditions, the mycelium mat grew on the surface of the liquid medium like on the surface of an agar medium. The mycelium was recovered at different time intervals (for up to 48 h), washed three times each with 100 ml of water, lyophilized, and the freeze dried material was quantified.

The amount of glucose present in the culture medium (after 48 h growth at 30°C) was measured by the O-toluidine method of Dobowski (Dawes *et al*., 1971).

Microsphere adhesion assay

To test the surface hydrophobicity of the mycelial mat, we used the microsphere adhesion assay. Sulfate yellow polystyrene latex microspheres (0.806 μm, Sigma) were used because they have a low negative charge density, with > 90% of the surface available for hydrophobic interactions (Hazen and Hazen, 1987). StA and ShS cultures were washed in 0.1 M KNO_3 pH 6.5 and mixed with an equal volume of microspheres (10^9 ml^{-1}). The mixture was vortexed for 30 s and extensively washed with the KNO_3 solution. The adhesion of the microspheres to the hyphae was observed under a fluorescent microscope (excitation 470 nm, emission 505 nm).

Scanning confocal laser and inverted wide-field epifluorescence microscopy

Microscopic analysis of growth on solid medium and image acquisition were performed on an upright scanning confocal laser microscope (LSM 510, version3.2, Zeiss, Germany) and an inverted wide-field epifluorescence microscope system (Carl Zeiss, Germany). Analysis of the extracellular material from StA mycelium with a fluorescent probe was performed after dropping 100 μl of 10 μg ml^{-1} calcofluor white solution on the surface of the mycelium and incubating for 15 min at room temperature. Washing was not necessary and the StA sheet was observed directly using either confocal- or epifluorescence modalities. Image scanning was carried out using a blue diode 405 nm excitation/BP 420–480 nm emission.

TEM and cryo-SEM

For ultrastructure analysis, the mycelium was fixed overnight at 4°C in 2.5% glutaraldehyde in 0.1 M Na cacodylate buffer, post-fixed for 1 h in the same buffer containing 1% osmium tetroxide, then embedded in Spurr's resin (Phillips *et al*., 1992). All sections were stained with 4% uranyl acetate followed by 2.6% lead citrate, and observed under 80 kV in a Jeol transmission electron microscope (Jem 1010). For immunolabeling, the mycelium was fixed overnight at 4°C in 2% paraformaldehyde in 0.1 M sodium phosphate buffer, post-fixed for 1 h at 25°C in 2% paraformaldehyde and 0.1% glutaraldehyde in the same buffer, and embedded in K4M resin after repeated washing with 50 mM Ammonium chloride to quench aldehydes. Ultrathin sections were incubated for 30 min at 25°C with a protein block Aurion solution (Aurion, the Netherlands) and for 1 h with the monoclonal antibody EBA2 against *A. fumigatus* galactomannan (Stynen *et al*., 1992) at 0.3 μg per ml of IgM, or with an anti-α1,3 glucan purified rabbit polyclonal antiserum [kind gift of Dr Osumi, Women's University of Tokyo, Japan (Sugawara *et al*., 2003)] diluted 1:50 in TBG (50 mM Tris-HCl pH 7.6, 15 mM glycine). After several washes in TBG, thin sections were incubated, respectively, for 1 h at room temperature with anti-rat IgG goat antibodies coupled to 5 nm colloidal gold (Jackson, Cambs, England) 1/100 diluted, or an anti-rabbit F(ab′)2 goat antibodies coupled to 10 nm colloidal gold (BBI) 1/25 diluted. After several washes in TBG and TBS (50 mM Tris-HCl pH 7.6, 0.15 M NaCl), the grids were post-fixed with 1% glutaraldehyde in TBS for 10 min and observed at 80 kV in the Jeol transmission electron microscope. Control antibodies included the monoclonal antibodies EB-Y8 specific for *Yersinia enterocolitica*, O:8 for anti-galactomannan immunoassays (Stynen *et al*., 1992), and a pre-immune rabbit antiserum for anti-α1,3 glucan immunoassays.

StA and ShS mycelia were analysed with a JEOL JSM-6700F apparatus, which is an ultra-high-resolution field emission scanning electron microscope equipped with a cold-field-emission gun and a strongly excited conical lens. The secondary-electron-image resolution was 1 nm at 15 kV and 2.2 nm at 1 kV. Pieces of culture were frozen using a Gatan Alto 2500 cryo-stage and cryo-preparation chamber. The preparation conditions were as described in Paris *et al*. (2003). Cryo-fractures were performed in a cryo-preparation chamber with a cutter.

Sensitivity to antifungal compounds, desiccation and temperature

The effect of antifungal drugs on ShS and StA cultures of *A. fumigatus* was tested with a methodology adapted from Ramage and Lopez-Ribot (2005). Before the addition of antifungal drugs, StA and ShS mycelia were washed with sterile water and filtered under vacuum. Then, 6 mg (wet weight) of ShS mycelium or a 3-mm-diameter disk of the StA thallus was incubated with 250 μl of antifungal agents. Preliminary experiments demonstrated that these inocula were similar, both weighting

0.8 ± 0.1 mg when lyophilized. After incubation in the presence of the drug (see below), the mycelial was extensively washed with sterile water, and deposited on top of a GYE agar plate to determine viability. After 24 h at 37°C, the radius of the colony formed was measured and the MIC_{50} was determined as the minimal inhibitory concentration for which the growth radius of the colony was 50% those of the wild type.

Five antifungal drugs (two azoles, two polyenes and one echinocandin) were selected. Preliminary experiments have defined the range of concentrations to be tested: itraconazole 1–40 μg ml^{-1} in 0.1% DMSO; voriconazole 0.6–5 μg ml^{-1} in 0.1% DMSO; amphotericin B 25–200 μg ml^{-1} in 0.1% DMSO; nystatin 25–200 μg ml^{-1} in 0.1% DMSO; and caspofungin 0.125–1 μg ml^{-1} in water. Preliminary experiments have shown that the incubation conditions that gave the best discrimination between StA and ShS mycelia are 24 h at 25°C. Accordingly, all antifungal drugs except nystatin were incubated for 24 h with the StA and ShI mycelia. A shorter time of incubation was used for nystatin (2 h at 37°C) because under the concentrations tested, a longer incubation time killed the fungus.

Sensitivity to dessication was tested by leaving a 24 h StA and a 30 h ShS mat of mycelium at room temperature (21–24°C) for up to 1 month and deposited on top of a GYE agar plate at 37°C to measure viability.

Resistance to heat was tested by incubating a 24 h StA and a 30 h ShS culture at 60°C for 6 h and transferring the plate to 37°C.

Melanin determination

Mycelial melanin was extracted as previously described (Beauvais *et al.*, 2005). Briefly, the mycelium was collected by filtration, washed with water and lyophilized. Freeze dried material (150 mg) was degraded for 14 h at 30°C in 10 mg ml^{-1} Glucanex (Novo), denatured for 14 h at 25°C in 4 M guanidine thiocyanate, incubated for 14 h at 37°C in proteinase K (1 mg ml^{-1}, Sigma) and boiled for 1.5 h at 160°C in 6 N HCl to isolate melanin from other cell wall components as described by Rosas *et al.* (2000).

Cell wall analysis

Monosaccharide components of the cell wall polysaccharides were analysed by gas chromatography after separation of alkali-soluble and alkali-insoluble fractions (Beauvais *et al.*, 2005). β and α1,3 glucans were quantified by measuring the amount of reducing sugar released by recombinant β and α1,3 glucanases (Beauvais *et al.*, 2005).

Extraction of extracellular material

The extracellular material was extracted by gently rubbing the surface of the mycelium from a StA culture with water (5 ml per 20 ml of agar culture) using an inoculation spreader (Sarstedt). In contrast to other methods (stirring or vortexing the mycelial mats), this method removed the matrix without damaging the hyphae.

Mono-, polysaccharides and polyols of the extracellular material were analysed. Soluble monosaccharides and polyols were determined on a HPLC Aminex HPX-87H Column for the organic acid analysis (300 × 7.8 mm, Bio-Rad) using 10 mM H_2SO_4 as eluant at a flow rate of 0.6 ml min^{-1} and detected with a refractometer. Polysaccharides were precipitated with 4 volumes ethanol and analysed by gas chromatography after hydrolysis by 4 N trifluoroacetic acid 4 h at 100°C, reduction by 10 mg ml^{-1} Na_2BH_4 in 0.1 M NH_4OH, and peracetylation as described previously (Beauvais *et al.*, 2005). β and α1,3 glucans were determined as above.

Proteins were quantified with the Bradford procedure using a commercial kit from Bio-Rad and were analysed by SDS-PAGE gel electrophoresis using 10% (w/v) acrylamide separating gels (Laemmli, 1970). Proteins were electrotransferred on nitrocellulose membranes. Major *A. fumigatus* antigens (DPPV, catalase and ribonuclease) were detected by Western blots using an anti-DPPV hyper-immune mouse serum, anti-catalase and anti-ribonuclease hyperimmune rabbit sera (Paris *et al.*, 1993; Beauvais *et al.*, 1997; Calera *et al.*, 1997). All sera and their respective peroxidase-conjugated anti-IgG (H+L) antibodies (Sigma) were diluted 1/1000. Band detection was performed using the ECM chemoluminescence system of Amersham.

Hydrophobin gene expression

To follow the expression of hydrophobins, total RNA was extracted from 10 ml of StA and ShS cultures. The age of the cultures was 24 h for StA and 30 h for ShS at 30°C as the mycelia had a similar total growth at that time (see *Results*). The cultures were washed with water and the mycelium was disrupted with a pestle in a frozen mortar in liquid nitrogen in the presence of 1 ml of Trizol. RNA extraction was undertaken following the Trizol protocol (http://www.invitrogen.com/search.cfm), with minor modifications: the samples were incubated for 5 min at room temperature and centrifuge at 12 000 *g* for 5 min at 4°C before addition of the chloroform (0.2 ml). The RNA was first precipitated with 0.25 ml of isopropanol and 0.25 ml of SSC (0.8 M Na citrate, 1.2 M NaCl), washed twice with 70% ethanol, air-dried and suspended in 0.5 ml of H_2O. A second precipitation was undertaken by adding 0.5 ml of LiCl buffer (4 M LiCl, 20 mM Tris-HCl pH 7.5, 10 mM EDTA) for at least 1 h at –20°C. RT-PCR assays were performed according to the manufacturer's instructions (Superscript One-Step RT-PCR with Platinum Taq, Invitrogen: RT step: 50°C 23 min, denaturation step: 94°C 2 min, 35 cycles PCR: 94°C 15 s, 55°C 30 s, 70°C 1 min, final elongation step: 72°C 8 min), using the total RNA and primers determined for the hydrophobin genes (http://www.cadre.man.ac.uk/Aspergillus_fumigatus/). Primers used for the PCR assay were:

RODA (Afu5g09580):	5′primer: GCGCTGCTGTCCTCGCTTTG
	3′primer: AGGATAGAACCAAGGGCAATG
RODB (Afu1g17250):	5′primer: TTGTCTCTCTCCTCGCTGCC
	3′primer: GAGTCGAGAGCAACGCAGGC
RODC (Afu8g07060):	5′primer: TATCCCGGAGTATCGCAGTC
	3′primer: ACTGACACCGACACCAGATG
RODD (Afu5g01490):	5′primer: ATGCCTCATTTCTGCCTTAT
	3′primer: GGCCATGATGACGAGAGAAG
RODE (Afu8g05890):	5′primer: TCCACGACCAGAACATCTTTC
	3′primer: CAGCCCAGAACAATGAGRCC
RODF (Afu5g03280):	5′primer: CCCTCGCTACACTCTCAACC
	3′primer: ATACTCCGAAAACCGCCTCT

Acknowledgements

We thank very much Professor Osumi (Women's University of Tokyo, Japan) and B. Humbel (Utrecht University, the Nether-

lands) for the kind gift of the α1,3 glucan antibody, A. Brakhage (Friedrich-Schiller-University, Jena, Germany) for the kind gift of the ATCC 46645 strain, S. Shorte as the head of the Dynamic Imagery Platform of the Pasteur Institute and D. Perlin (Public Health Research Institute, Newark, USA) and R. Calderone (Georgetown University Medical Center, Washington, USA) for reading of the manuscript.

References

Anwar, H., Strap, J.L., and Costerton, J.W. (1992) Establishment of aging biofilms: possible mechanism of bacterial resistance to antimicrobial therapy. *Antimicrob Agents Chemother* **36:** 1347–1351.

Baillie, G.S., and Douglas, L.J. (2000) Matrix polymers of *Candida* biofilms and their possible role in biofilm resistance to antifungal agents. *J Antimicrob Chemother* **46:** 397–403.

Beauvais, A., Monod, M., Debeaupuis, J.P., Diaquin, M., Kobayashi, H., and Latgé, J.P. (1997) Biochemical and antigenic characterization of a new dipeptidyl-peptidase isolated from *Aspergillus fumigatus*. *J Biol Chem* **272:** 6238–6244.

Beauvais, A., Maubon, D., Park, S., Morelle, W., Tanguy, M., Huerre, M., *et al.* (2005) Two alpha(1-3) glucan synthases with different functions in *Aspergillus fumigatus*. *Appl Environ Microbiol* **71:** 1531–1538.

Brooun, A., Liu, S., and Lewis, K. (2000) A dose–response study of antibiotic resistance in *Pseudomonas aeruginosa* biofilms. *Antimicrob Agents Chemother* **44:** 640–646.

Calera, J.A., Paris, S., Monod, M., Hamilton, A.J., Debeaupuis, J.P., Diaquin, M., *et al.* (1997) Cloning and disruption of the antigenic catalase gene of *Aspergilus fumigatus*. *Infect Immun* **65:** 4718–4724.

Chandra, J., Kuhn, D.M., Mukherjee, P.K., Hoyer, L.L., McCormick, T., and Ghannoum, M.A. (2001) Biofilm formation by the fungal pathogen *Candida albicans*: development, architecture, and drug resistance. *J Bacteriol* **183:** 5385–5394.

Dawes, E.A., MacGill, D.J., and Midgley, M. (1971) Analysis of fermentation products. In *Methods in Microbiology*, Vol. 6A. Norris, J.R., and Ribbons, P.W. (eds). New York: Academic Press, pp. 53–215.

Donlan, R.M., and Costerton, J.W. (2002) Biofilms: survival mechanisms of clinically relevant microorganisms. *Clin Microbiol Rev* **15:** 167–193.

Douglas, L.J. (2003) *Candida* biofilms and their role in infection. *Trends Microbiol* **11:** 30–36.

Garcia-Sanchez, S., Aubert, S., Iraqui, I., Janbon, G., Ghigo, J.M., and d'Enfert, C. (2004) *Candida albicans* biofilms: a developmental state associated with specific and stable gene expression patterns. *Eukaryot Cell* **3:** 536–545.

Gerber, L.D., Kodukula, K., and Udenfriend, S. (1992) Phosphatidylinositol glycan (PI-G) anchored membrane proteins. Amino acid requirements adjacent to the site of cleavage and PI-G attachment in the COOH-terminal signal peptide. *J Biol Chem* **267:** 12168–12173.

Hazen, K.C., and Hazen, B.W. (1987) A polystyrene microsphere assay for detecting surface hydrophobicity variations within *Candida albicans* populations. *J Microbiol Methods* **6:** 289–299.

Laemmli, U.K. (1970) Cleavage of structural proteins during the assembly of the head of bacteriophage T4. *Nature (London)* **227:** 680–685.

Latgé, J.P. (2003) *Aspergillus fumigatus*, a saprophytic pathogenic fungus. *Mycologist* **17:** 56–61.

Lewis, K. (2001) Riddle of biofilm resistance. *Antimicrob Agents Chemother* **45:** 999–1007.

Linder, M.B., Szilvay, G.R., Nakari-Setala, T., and Penttila, M.E. (2005) Hydrophobins: the protein-amphiphiles of filamentous fungi. *FEMS Microbiol Rev* **29:** 877–896.

Mack, D., Fischer, W., Krokotsch, A., Leopold, K., Hartmann, R., Egge, H., and Laufs, R. (1996) The intercellular adhesin involved in biofilm accumulation of *Staphylococcus epidermidis* is a linear beta-1,6-linked glucosaminoglycan: purification and structural analysis. *J Bacteriol* **178:** 175–183.

Maira-Litran, T., Allison, D.G., and Gilbert, P. (2000) An evaluation of the potential of the multiple antibiotic resistance operon (*mar*) and the multidrug efflux pump *acrAB* to moderate resistance towards ciprofloxacin in *Escherichia coli* biofilms. *J Antimicrob Chemother* **45:** 789–795.

Martinez, L.R., and Casadevall, A. (2006) Susceptibility of *Cryptococcus neoformans* biofilms to antifungal agents *in vitro*. *Antimicrob Agents Chemother* **50:** 1021–1033.

Paris, S., Monod, M., Diaquin, M., Lamy, B., Arruda, L.K., Punt, J.P., and Latgé, J.P. (1993) A transformant of *Aspergillus fumigatus* deficient in the antigenic cytotoxin ASPF1. *FEMS Microbiol Lett* **111:** 31–36.

Paris, S., Debeaupuis, J.P., Crameri, R., Cary, M., Charlès, F., Prévost, M.C., *et al.* (2003) Conidial hydrophobins of *Aspergillus fumigatus*. *Appl Environ Microbiol* **69:** 1581–1588.

Phillips, D.M., Pearce-Pratt, R., Tan, X., and Zacharopoulos, V.R. (1992) Association of mycoplasma with HIV-1 and HTLV-I in human T lymphocytes. *AIDS Res Hum Retroviruses* **8:** 1863–1868.

Ramage, G., and Lopez-Ribot, J.L. (2005) Techniques for antifungal susceptibility testing of *Candida albicans* biofilms. *Methods Mol Med* **118:** 71–79.

Ramage, G., Bachmann, S., Patterson, T.F., Wickes, B.L., and Lopez-Ribot, J.L. (2002) Investigation of multidrug efflux pumps in relation to fluconazole resistance in *Candida albicans* biofilms. *J Antimicrob Chemother* **49:** 973–980.

Richter, M., Willey, J.M., SüBmuth, R., Jung, G., and Hiedler, H.P. (1998) Streptofactin, a novel biosurfactant with aerial mycelium inducing activity from *Streptomyces tendae* Tü 901-8c. *FEMS Microbiol Lett* **163:** 165–171.

Rosas, A.L., Nosanchuk, J.D., Feldmesser, M., Cox, G.M., McDade, H.C., and Casadevall, A. (2000) Synthesis of polymerized melanin by *Cryptococcus neoformans* in infected rodents. *Infect Immun* **68:** 2845–2853.

Samaranayake, Y.H., Ye J., Yau, J.Y.Y., Cheung, B.P.K., and Samaranayake, L.P. (2005) *In vitro* method to study antifungal perfusion in *Cancida albicans*. *J Clin Microbiol* **43:** 818–825.

Sarfati, J., Monod, M., Recco, P., Sulahian, A., Pinel, C., Cardolfi, E., *et al.* (2006) Recombinant antigens as diagnostic markers for aspergillosis. *Diagn Microbiol Infect Dis* **55:** 279–291.

Stynen, D., Sarfati, J., Goris, A., Prévost, M.C., Lesourd, M.,

Kamphuis, H., *et al.* (1992) Rat monoclonal antibodies against galactomann. *Infect Immun* **60:** 2237–2245.
Sugareva, V., Hartl, A., Brock, M., Hubner, K., Rohde, M., Heinekamp, T., and Brakhage, A.A. (2006) Characterisation of the laccase-encoding gene *abr2* of the dihydroxynaphthalene-like melanin gene cluster of *Aspergillus fumigatus*. *Arch Microbiol* **186:** 345–355.
Sugawara, T., Sato, M., Takagi, T., Kamasaki, T., Ohno, N., and Osumi, M. (2003) *In situ* localization of cell wall alpha-1,3-glucan in the fission yeast *Schizosaccharomyces pombe*. *J Electron Microsc (Tokyo)* **52:** 237–242.
Tekaia, F., and Latgé, J.P. (2005) *Aspergillus fumigatus*: saprophyte or pathogen? *Curr Opin Microbiol* **8:** 385–392.
Tillotson, R.D., Wosten, H.A., Richter, M., and Willey, J.M. (1998) A surface active protein involved in aerial hyphae formation in the filamentous fungus *Schizophillum commune* restores the capacity of a bald mutant of the filamentous bacterium *Streptomyces coelicolor* to erect aerial structures. *Mol Microbiol* **30:** 595–602.
Wösten, H.A., and de Vocht, M.L. (2000) Hydrophobins, the fungal coat unravelled. *Biochim Biophys Acta* **1469:** 79–86.
Wösten, H.A., Bohlmann, R., Eckerskorn, C., Lottspeich, F., Bolker, M., and Kahmann, R. (1996) A novel class of small amphipathic peptides affect aerial hyphal growth and surface hydrophobicity in *Ustilago maydis*. *EMBO J* **15:** 4274–4281.
Wösten, H.A., van Wetter, M.A., Lugones, L.G., van der Mei, H.C., Busscher, H.J., and Wessels, J.G. (1999) How a fungus escapes the water to grow into the air. *Curr Biol* **9:** 85–88.